WILEY | Hindawi

Research Article

A Study of Support Characteristics of Collaborative Reinforce System of U-Steel Support and Anchored Cable for Roadway under High Dynamic Stress

Qizhou Wang,[1,2] Haiwang Ye,[1,2] Ning Li [1,2] Xiuwen Chi,[1,2] Wenbing Xie,[3] Dongfang Chen,[1,2] Shengguo Jing,[3] and Tao Lei[1,2]

[1]*Key Laboratory of Hubei Province for Mineral Resources Processing and Environment, Wuhan University of Technology, Wuhan Hubei 430070, China*
[2]*School of Resources and Environmental Engineering, Wuhan University of Technology, Wuhan Hubei 430070, China*
[3]*State Key Laboratory of Coal Resources and Safe Mining, China of Mining and Technology, Xuzhou Jiangsu 221116, China*

Correspondence should be addressed to Ning Li; 13875910191@163.com

This paper presents a comprehensive study of the support effect and characteristics of a collaborative reinforce system of U-steel support and anchored cable (USS-AC) for roadway under high dynamic stress in a coal mine in China. The deformational behavior of the roadway and the load characteristics of reinforcing elements were measured in real time and analyzed. A numerical simulation study has also been conducted to identify the interaction of the reinforcing elements to the surrounding rock under dynamic load. The research results suggest that the stress distribution of roadway surrounding rock could be changed and that residual strength of the surrounding rock near opening could be increased by using USS-AC. Based on the action of anchored cable, the moment distribution of U-steel support is optimized. The load capacity and nondeformability of the U-steel support are promoted. And the global stability of U-steel support is enhanced so as to achieve the goal of high supporting resistance. When the deformation stress of the surrounding rock is higher, the U-steel support deforms as the surrounding rock. The two side beams and the overlapping parts of U-steel support suffer the highest deformation stress. As a result, the anchored cable provides higher reaction force for the previous locations of the U-steel support in order to prevent deformation of support towards to excavation. As an integral structure, the U-steel support is confined to a limited deformation space under the action of anchored cable. The larger deformation is released through sliding motion of the overlapping parts so as to reach the ultimate of high supporting resistance of USS-AC.

1. Introduction

Strata control of roadways developed in soft rock under high in situ stress has become a challenging problem due to increasing mining depth in recent years. It was reported that more than 80% roadways experienced dynamic pressure in the central and eastern China [1, 2]. Numerous research works related to ground support technology for soft rock roadway under high dynamic pressure have been conducted. Among them, active supports of rock bolts or cables have been proposed [3–7]. Besides, a combination of active support of rock bolts and passive support of U-steel has been

developed and identified as an effective manner for such geo-conditions [8–10]. For a case study of the -720 south-wing track haulage roadway under dynamic pressure in Renlou Coal Mine in China, U-steel supports, U-steel support wall thickness grouting combination support, and bolting support with wire mesh have failed to decrease the intense deformation of surrounding rock of the roadway. Aiming at such geological condition of soft rock roadways under high-stress, a collaborative reinforce system of U-steel support and anchored cable (USS-AC) was proposed and adopted [9, 10]. The field test indicates that USS-AC is an effective approach to reduce the displacement of the
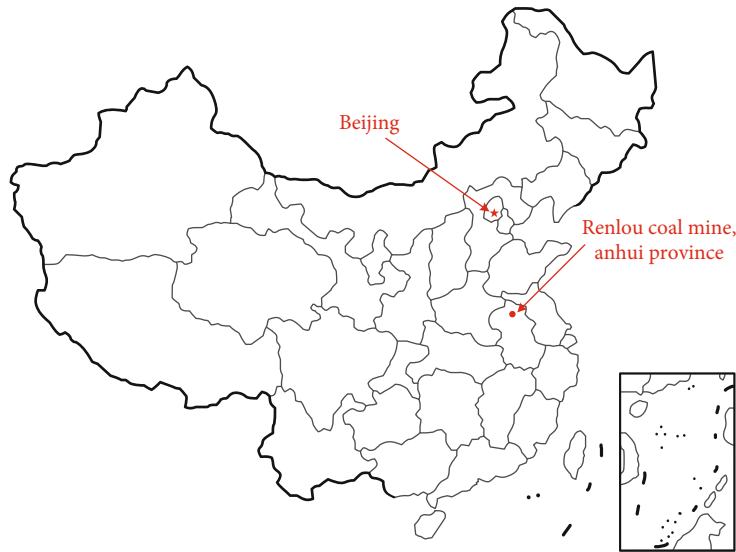
Figure 1: Location of the Renlou Coal Mine.

surrounding rock of the haulage roadway. Load characteristics of U-steel support and anchored cable of USS-AC were analyzed, respectively, by theoretical calculations under static stress [9–15]. However, the transformation law of actual load on U-steel support has not been monitored and obtained with suffering dynamic stress from the beginning to the end of excavation of workface. Therefore, the collaborative interaction between U-steel support and anchored cable of USS-AC could not be described.

For solving the previous issues, optimizing action of stress distribution of surrounding rock under USS-AC and bending moment of U-steel support with collaborative anchored cables were analyzed by a numerical simulation method to reveal the interaction mechanism of USS-AC. Specific parameters of USS-AC were proposed for the field test in Renlou Coal Mine. Meanwhile, actual load of U-steel support and anchored cables respective as well as displacement of surrounding rock of test roadway were monitored by a filed measurement method. The deformation of the surrounding rock and its corelationship to the actual load of USS-AC were disclosed by using of test data. The increasing effect of anchored cables for U-steel support bearing capacity and structural stability was described.

2. Project Overview

The project was at Renlou Coal Mine in the north of Anhui Province of China (Figure 1). The -720 south-wing track haulage roadway was the main channel for pedestrians and ventilation of the mine. The shape of roadway section was a straight wall semicircular arch with a height of 3.9 m and a width of 5.0 m. The roadway with overburden depth 750 m was arranged in the floor strata of coal seam $NO.8_2$ at a perpendicular distance of 43 m-70 m from coal seam $NO.7_2$ and 20 m-50 m from coal seam $NO.8_2$. The relative plane location relationship between the -720 south-wing track haulage roadways with working face $II7_214$ is given in Figure 2.

The -720 south-wing track haulage roadway was excavated in siltstone and mudstone. The side walls of roadway were mudstone, and the arch roof was siltstone, respectively. The rock of immediate roof was a 2.5 m thick siltstone, which was overlaid by a main roof of fine sandstone with a thickness of 5.0 m.

A combined bolting method, with bolts, cables, and steel bar truss, was conducted in the -720 south-wing track haulage roadway. As shown in Figure 3, the deformation of haulage roadway was insignificant to satisfy the operation requirements without the influence of dynamic pressure of working face $II7_214$. However, the previous method failed to restrain the deformation of roadway that roof-to-floor convergence reached 0.8 m with the side-to-side convergence up to 1.0 m under excavation of working face. The roadway deformation was so severe that the surrounding rock became loose and broken with a strength reduction. Therefore, in the service period of the roadway, it was severely impacted by dynamic stress due to mining activity of working face $II7_214$.

3. Functional Mechanism of USS-AC

3.1. Numerical Modelling. USS-AC was divided into two segments. The U-steel support was the primary and basic component to support the loose rock mass near to the excavation of roadway. The second part consisted of anchored cables and joists that linked cables with U-steel supports and transmitted pretension of cables to U-steel supports. The Flac^{2D} model was built to, respectively, analyze a stress distribution law of roadway surrounding rock and a bending moment variation law inside of U-steel.

The numerical model has a length of 80 m and a height of 80 m with element size 0.2 m × 0.2 m that Mohr-Coulomb constitutive model in FLAC^{2D} was used to simulate the mechanical behaviors of rocks. The model size and parameters of rocks are illustrated in Figure 4. The normal displacement of the four lateral surfaces and
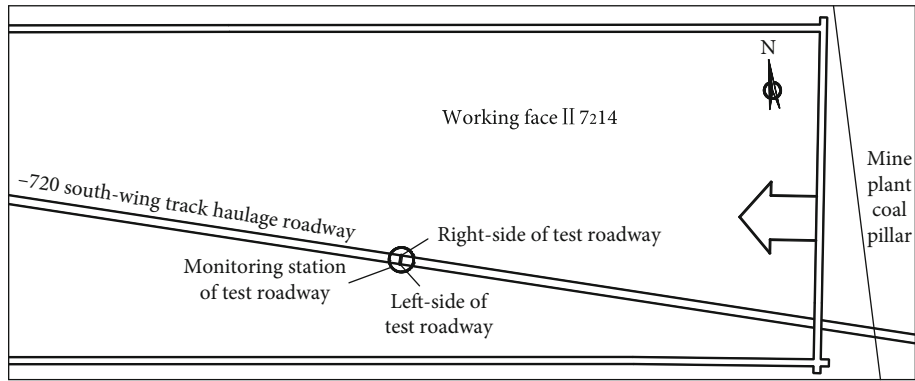
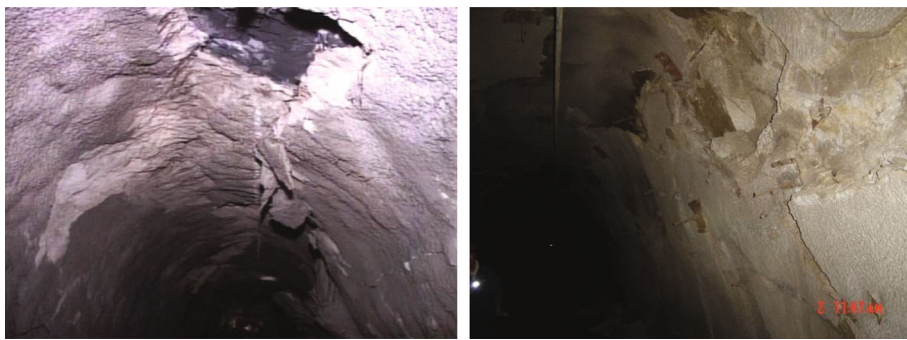FIGURE 2: Plane location relationship between -720 south-wing track haulage roadway and working face II7214.

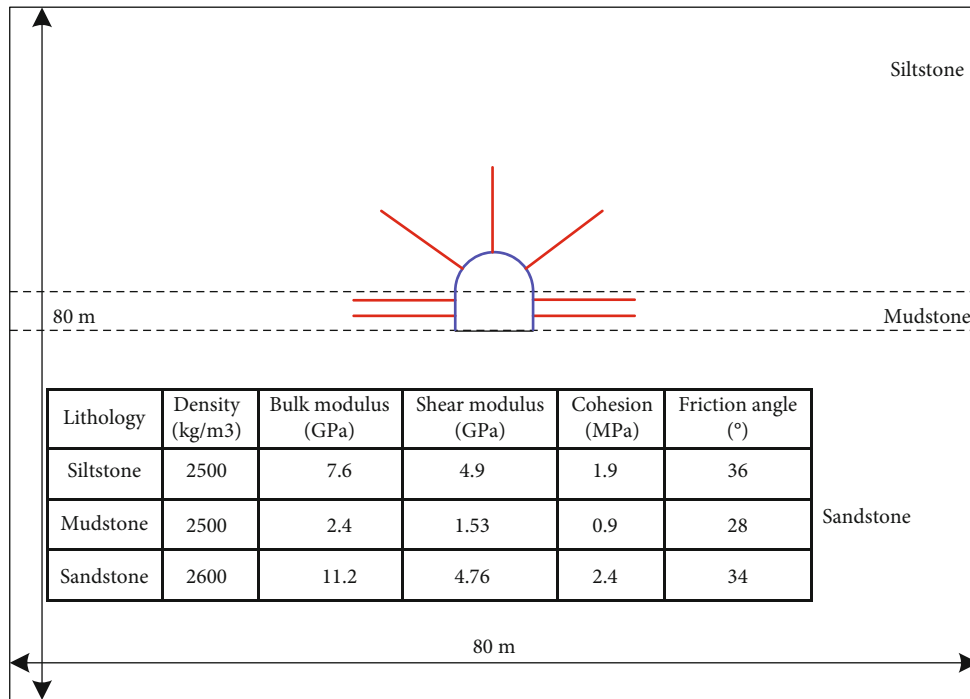
FIGURE 3: Deformation characteristics of haulage roadway.

Lithology	Density (kg/m3)	Bulk modulus (GPa)	Shear modulus (GPa)	Cohesion (MPa)	Friction angle (°)
Siltstone	2500	7.6	4.9	1.9	36
Mudstone	2500	2.4	1.53	0.9	28
Sandstone	2600	11.2	4.76	2.4	34

FIGURE 4: The model size and parameters of rocks.

the bottom surface of the model were fixed to be zero. The stress ($\varepsilon_{zz} = \varepsilon_{xx} = \varepsilon_{yy} = 18$ MPa) was applied on the top surface of model to simulate the overburden rock load in the condition of initial stress. A beam unit was adopted to simulate U-steel support. In addition, a cable unit was used to simulate the anchored cable with a length of

6.5 m. And the two support units were linked by slave command in Flac^{2D}.

The implementation was divided into three steps: firstly, excavating the roadway region after initial equilibrium of model. And then, support units were set, and the top stress of model was changed into 21.6 MPa to simulate the extra stress due to excavation activity of working face.

3.2. Numerical Modelling Results. Figure 5 shows vertical stress distribution law of the roadway surrounding rock after using two different support ways that U-steel support and USS-AC are adopted, respectively.

It can be seen that the stress condition of the roadway surrounding rock is significantly optimized by using USS-AC. Compared with the roadway using a U-steel support, the development scope of low-stress of the surrounding rock is obviously reduced, while the vertical stress of the surrounding rock near to the excavation space of the roadway is generally increased. According to the research results [3, 16, 17], the residual strength of the rock mass near the excavation space of roadway is greatly increased to enhance the itself-bearing capacity due to increase of confine pressure in broken and fractured rock mass of roadway. Therefore, the confine pressure in fractured zone of test roadway is raised by USS-AC to increase the residual strength of the rock mass in the previous zone.

The load bearing capacity of the rock mass at a deep zone could be used by an active supporting effect of the anchored cable that links the U-steel with the deep rock mass of roadway. On the one hand, the stress concentration zone at the deep part in surrounding rock of the roadway was decreased by more than 50%. The bearing load of the rock mass at the deep part is reduced, and it was kept stable at the same time. On the other hand, the stress in the rock mass at the anchoring end of inside the anchored cable is significantly increased under the function of anchoring to enhance the strength and stiffness of rock mass at the deep part. The support and rock combining bearing structure that has been linked cables with U-steel by joist is formed and affords a large load to provide a higher deformation resistance.

Furthermore, the previous research results [9, 11, 12] showed that the bearing capacity of arch beam on the top of U-steel support is greater than that of side beam. As shown in Figure 6(a), because of poor interaction between U-steel support and surrounding rock near the excavation space of roadway, the load of arch beam is lower even zero in an actual bearing process. However, the overlap part and side beam bear larger load. Therefore, the arch beam of U-steel support is in the condition which bears low actual load and wastes the high resistance to the rock mass. On the contrary, the actual load of side beam is greater than the upper limit of its supporting resistance to create a larger bending moment in the transverse plane of the side beam center line. The load distribution law and bending moment feature of U-steel support generate a phenomenon that side beam is the first place of destruction and losing stability to result in difficultly using the high resistance and great strength of the arch beam.

The bending moment of U-steel support is shown in Figure 6(b) after applying USS-AC. The bending moment of arch beam is changed from 4 N·m to 1.21×10^3 N·m, while that of side beam declines from 7.12×10^4 N·m to 3.64×10^4 N·m. So, the bearing characteristics of U-steel support are optimized to reduce the bending moment of side beam and enlarge that of arch beam owing to anchored cables. The reduction of load difference between the arch beam and side beam is accomplished to reinforce the global stability of U-steel support.

4. The Technology Parameters of USS-AC

According to the geological condition of the -720 south-wing track haulage roadway and excavation arrangement of working face II7$_2$14 at the Renlou Coal Mine, collaborative supporting technology of USS-AC was adopted in the field test. The specific scheme with supporting parameters is shown in Figure 7.
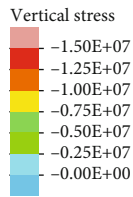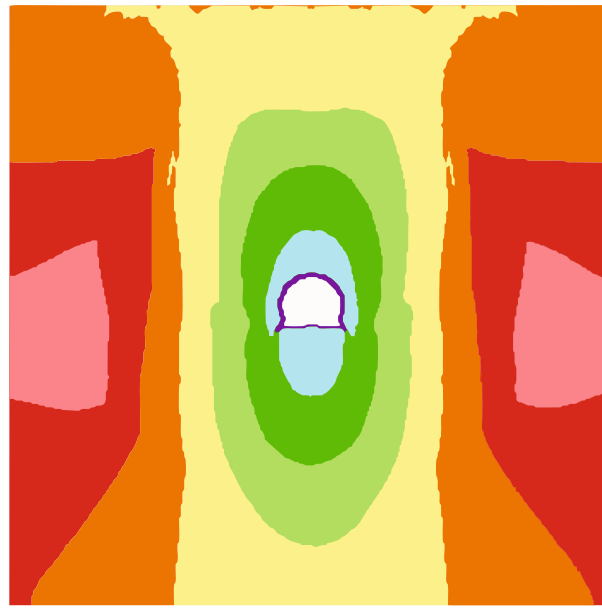
The parameters of U-steel support are evaluated as follows: the type of U-steel is 36# in Chinese standard. The U-steel support which is assembled by one arch beam on the top and two side beams is set as a main supporting manner with a spacing of 0.5 m. The length of arch beam is 6.13 m and overlapped in its two ends by side beam with a length of 3.54 m for each side. Three suits of locking devices by nuts are used in compressing each overlapping part with a length of 0.54 m.

The cable anchoring parameters are evaluated as follows: the diameter of anchored cable is 17.8 mm with a length of 6 m. Three anchored cables per row are installed in the center line of arch beam and two overlapping parts. Two anchored cables per row are installed in the right side beam with a row spacing of 1 m. One anchored cable per row is installed in the left side beam. The row-to-row distance of anchored cables is 1 m. And all cables are perpendicular to the surface of U-steel. Resin capsules are used to anchor the front part of the cables in the process of installing. The U-steel support is linked with anchored cables by a joist with a length of 0.8 m that is processed by the H-steel. There is a hole with a radius of 0.015 m so that the anchored cables could pass through and preload it on the exterior surface of a joist. Then, pretension loads of 80 kN-100 kN are applied to the cables.
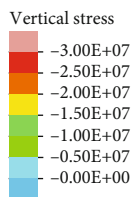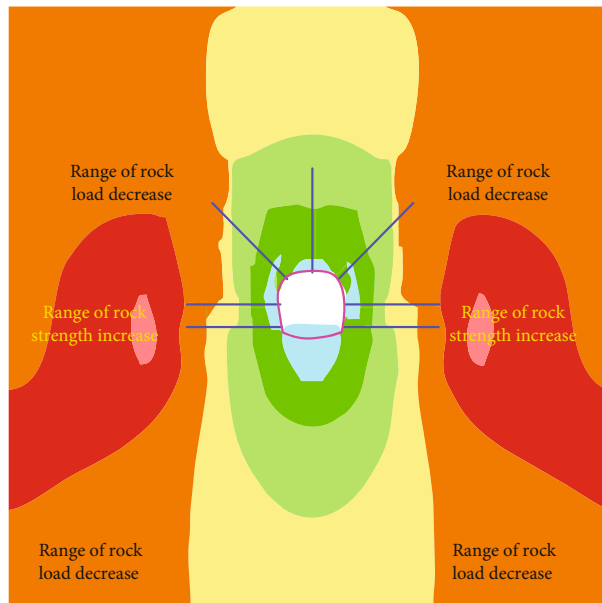
5. Field Monitoring Scheme

A monitoring station was set up in the -720 south-wing track haulage roadway and with a distance of 520 m in advance of working face II7$_2$14. The convergence of test roadway, actual load of the U-steel support, and load of exterior end of anchored cables were monitored from the beginning of dynamic influence of working face II7$_2$14 to the end.

5.1. Convergence of Test Roadway. The convergence of test roadway mainly refers to the displacement of the surrounding rock near to the excavation space of the roadway. A datum point was set up at the center of both sides, roof center, and floor center in a cross-section, respectively. At the

Vertical stress

- −1.50E+07
- −1.25E+07
- −1.00E+07
- −0.75E+07
- −0.50E+07
- −0.25E+07
- −0.00E+00

(a) U-steel support

Range of rock load decrease

Range of rock load decrease

Range of rock strength increase

Range of rock strength increase

Range of rock load decrease

Range of rock load decrease

Vertical stress

- −3.00E+07
- −2.50E+07
- −2.00E+07
- −1.50E+07
- −1.00E+07
- −0.50E+07
- −0.00E+00

(b) USS-AC

FIGURE 5: Vertical stress distribution law of roadway surrounding rock with different support methods.

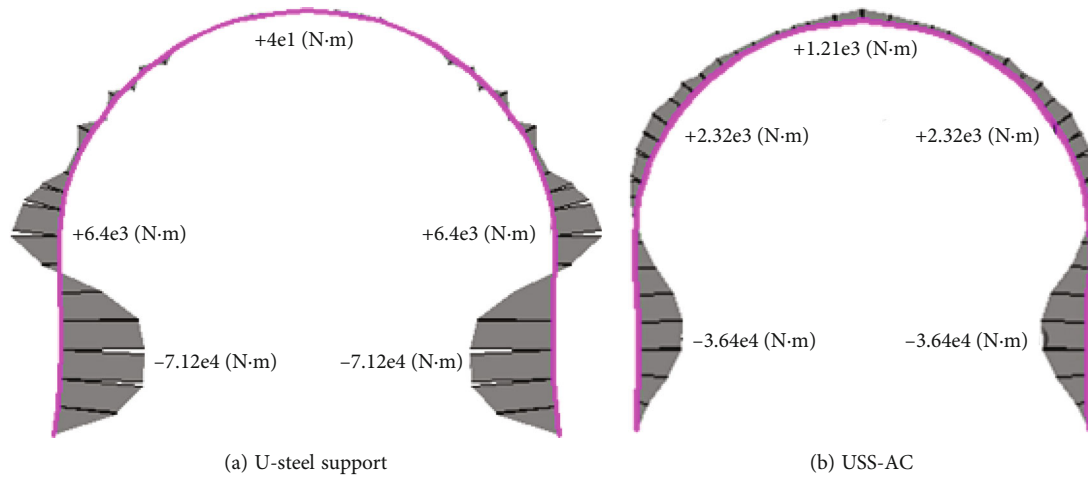(a) U-steel support

(b) USS-AC

FIGURE 6: Bending moment distribution law of U-steel support under different support methods.
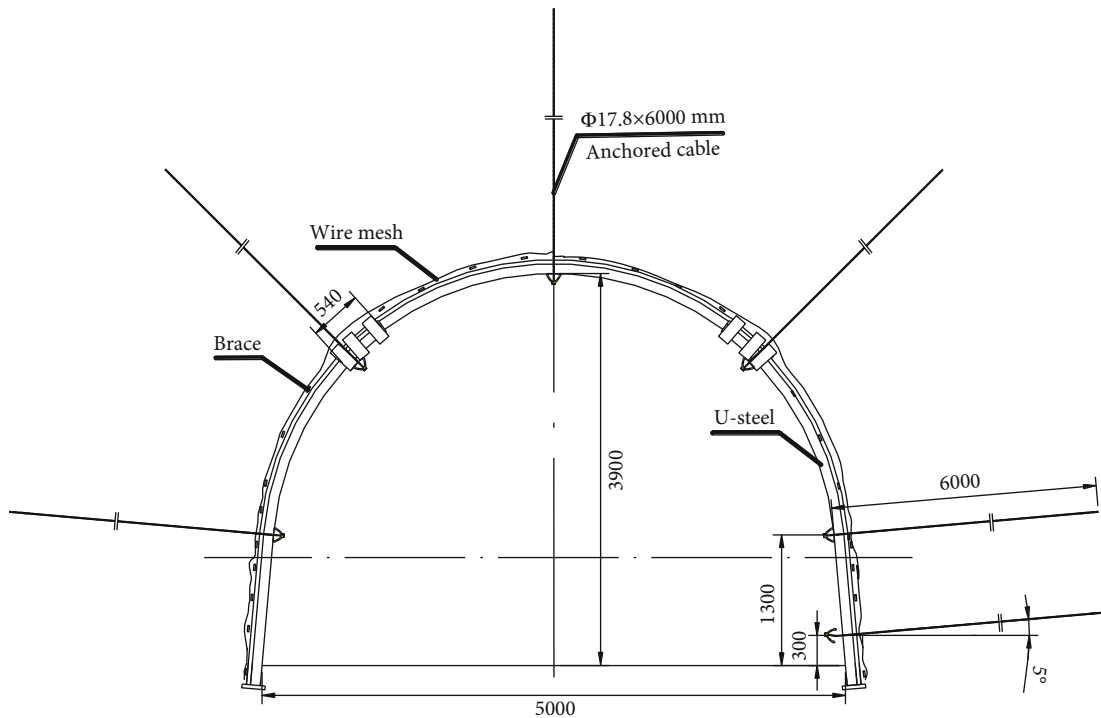

FIGURE 7: Layout of USS-AC with specific parameters in the case of test roadway.

beginning of monitoring process, the distances between datum points of the roof and floor and between datum points of both sides were measured by a laser distance measuring instrument as the initial value. And then, by subtracting each follow-up monitoring value from the initial value, the distance variation of roof-to-floor and side-to-side was determined and regarded as the convergence of test roadway.

5.2. Actual Load of the U-Steel Support. A hydraulic pressure pillow was adopted to survey the actual load of the U-steel support as shown in Figure 8. Before installing the hydraulic pressure pillow, a flat baseplate needed to be welded on the U-steel support. Further, a cover plate was installed between

the hydraulic pressure pillow and the rock mass to ensure the overall contact and guarantee the accuracy of test results. After installation completion, the display value of hydraulic pressure pillow was recorded.

5.3. Actual Load of Anchored Cable. A dynamometer named MGH-30 was adopted to conduct nondestructive monitoring for actual load of exterior end of anchored cable as Figure 9. Because of the supporting resistance of anchored cables applying on the surface of U-steel support by the device of joists, the pressure cells were installed among the joists and the anchorage devices so as to monitor the actual loads of anchored cables. During the operation, a specific number of preload were applied on the exterior end of
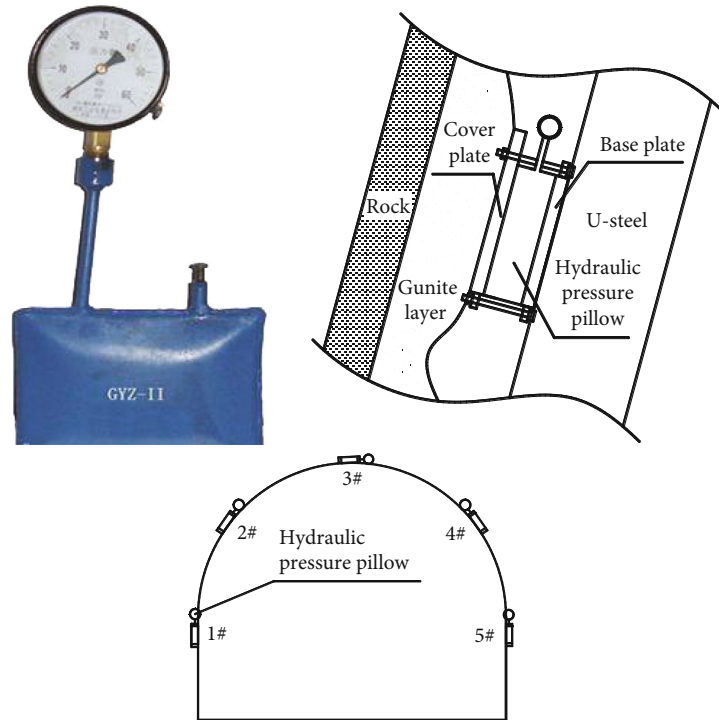
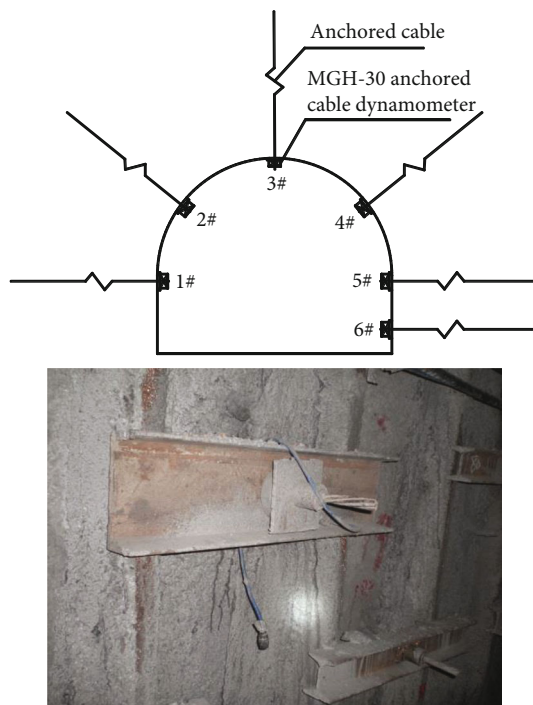FIGURE 8: Layout of hydraulic pressure pillow of U-steel support.

FIGURE 9: Layout and object diagram of anchored cable dynamometer.

anchored cable and recorded as the initial value. Afterwards, the hydraulic pressure pillows arranged on the U-steel support as well as the load of anchor cables were monitored at regular intervals.

6. Deformation Features of Test Roadway Subjected to Mining-Induced Stresses

The displacement feature of surrounding rock near to the excavation space of roadway was the composite indicator to reflect the stability of test roadway. Figure 10 shows the relationships among developing processes of displacement and its rate with the location of working face $II7_214$ from the beginning influence of the mining-induced stresses to the end. As shown in Figure 10, the negative value of the abscissa refers to the horizontal distance between the monitoring station and working face in the advancing direction of working face, while the positive value refers to the horizontal distance after that the working face has advanced through the monitoring station. The monitoring station is located about 200 m in front of the working face in the initial stage of measurement. And the deformation of roadway is gradually increased in a small rate without subjecting to mining-induced stresses. The deformation rate is 0.5 mm/d with a displacement sum of below 5 mm.

Thereafter, in the reduction process of distance between the monitoring station and working face from 180 m to 139 m, the displacement rate of roadway is converted into 0.3 mm/d with a displacement sum of below 10 mm. However, during the process of distance decreasing from 130 m to 39 m, the displacement rate of side-to-side and roof-to-floor is increased to 1 mm/d and above 0.5 mm/d, respectively. The displacement variation extent of side-to-side was larger than that of roof-to-floor. The main reason lies in that the distance from the upper working face to the monitoring station is large so as that the stress disturbance of side wall of test roadway is bigger than that of roof under
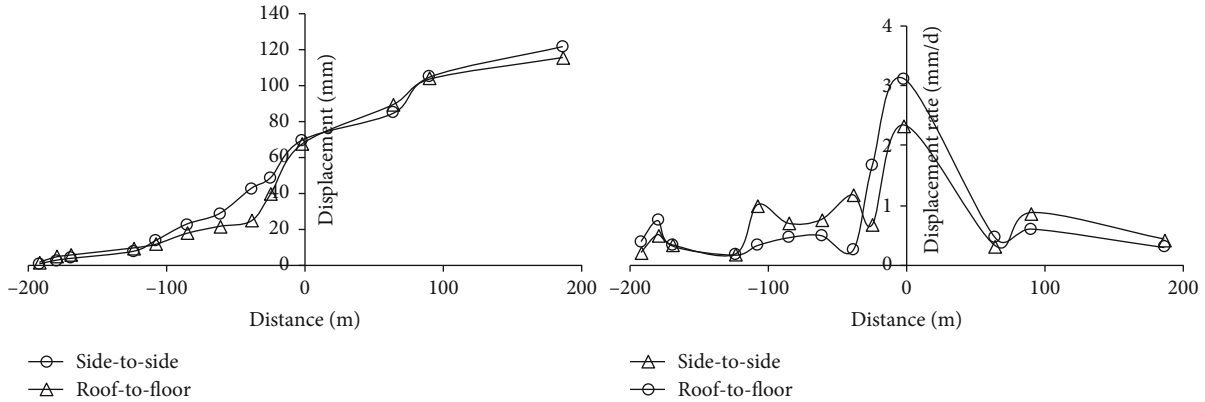
FIGURE 10: Displacement feature of test roadway subjected to mining-induced stresses.

mining-induced stresses. The integrity and strength of side wall rock are reduced significantly.

When the distance from the monitoring station to the working face is decreased from 39 m to 0 m, the displacement of surrounding rock is suddenly increased. The displacement rate of side-to-side is increased to 2.5 mm/d while that of roof-to-floor is increased to 3.2 mm/d. Although the displacement sum of roof-to-floor and that of side-to-side are approximately equal, the impacting degree of mining-induced stresses on the surrounding rock of roof is larger than that of side wall according to the displacement rate. That is because the working face is located right above the monitoring station so as to generate stronger impact on the roof of roadway. When the location of monitoring station has been advanced by the working face, the surrounding rock of roadway becomes more stable step-by-step along with the gradual increasing of distance between the working face and the monitoring station. Further, the displacement rate is gradually decreased to 0.5 mm/d.

7. Load Feature of USS-AC Subjected to Mining-Induced Stresses

7.1. Actual Load Feature of U-Steel Support. The actual load feature of U-steel support is shown as Figure 11. It can be seen that the variation of actual load is relatively small during the reduction process of distance between the monitoring station and the working face $II7_214$ from 300 m to 180 m in the advancing direction of working face. The load of left side beam center of U-steel support is about 60 kN, while that of the left overlapping part is about 55 kN. The load, about 30 kN, is observed in the pressure cell installed at the right side beam center, right overlapping part, and arch beam. In sum, the left part of U-steel support including left side beam and left overlapping part suffers larger load than that of other parts. When the monitoring station is 180 m from the working face, the load of the right overlapping part is suddenly increased to 75 kN without significant variation in other segments of support. The loads of both overlapping parts of the U-steel support are gradually increased in the reducing process of distance from 120 m to 110 m; in other words, the load of the left overlapping part and that of right overlapping part varied, 70 kN and 85 kN,
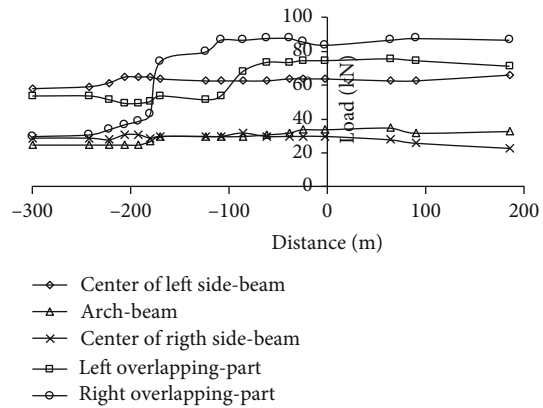

FIGURE 11: Developing process of actual load of U-steel support.

respectively. At the same time, the loads of other pressure cells of U-steel support were kept constant approximately.

7.2. Actual Load Features of Anchored Cables and USS-AC. The anchored cables directly contacted with the U-steel support via a joist. The supporting resistance of anchored cables is applied on the surface of U-steel support and transformed to the surrounding rock near the excavation of space of test roadway. In other words, the deformation features of U-steel support and sliding value of overlapping parts are reflected by the variation law of load in the exterior end of anchored cables. Meanwhile, the optimization actions of anchored cables on the U-steel support are obtained.

The relationship between the actual loads of USS-AC and convergence of roadway are shown in Figure 12. The developing process of actual loads of USS-AC is displayed undergoing the mining-induced stresses of working face $II7_214$.

As shown in Figures 12(a) and 12(b), the load of left side beam center of U-steel support is about 60 kN, while that of right side beam center is 30 kN. And the loads of the centers of both side beams are relatively stable under the mining-induced stresses. However, the loads of the anchored cables are increased and larger than those of U-steel support along with the deformation of surrounding rock of roadway. And

(a) The center of left side beam

(b) The center of right side beam

(c) Left overlapping part

(d) Right overlapping part

(e) Arch beam on the top of U-steel support

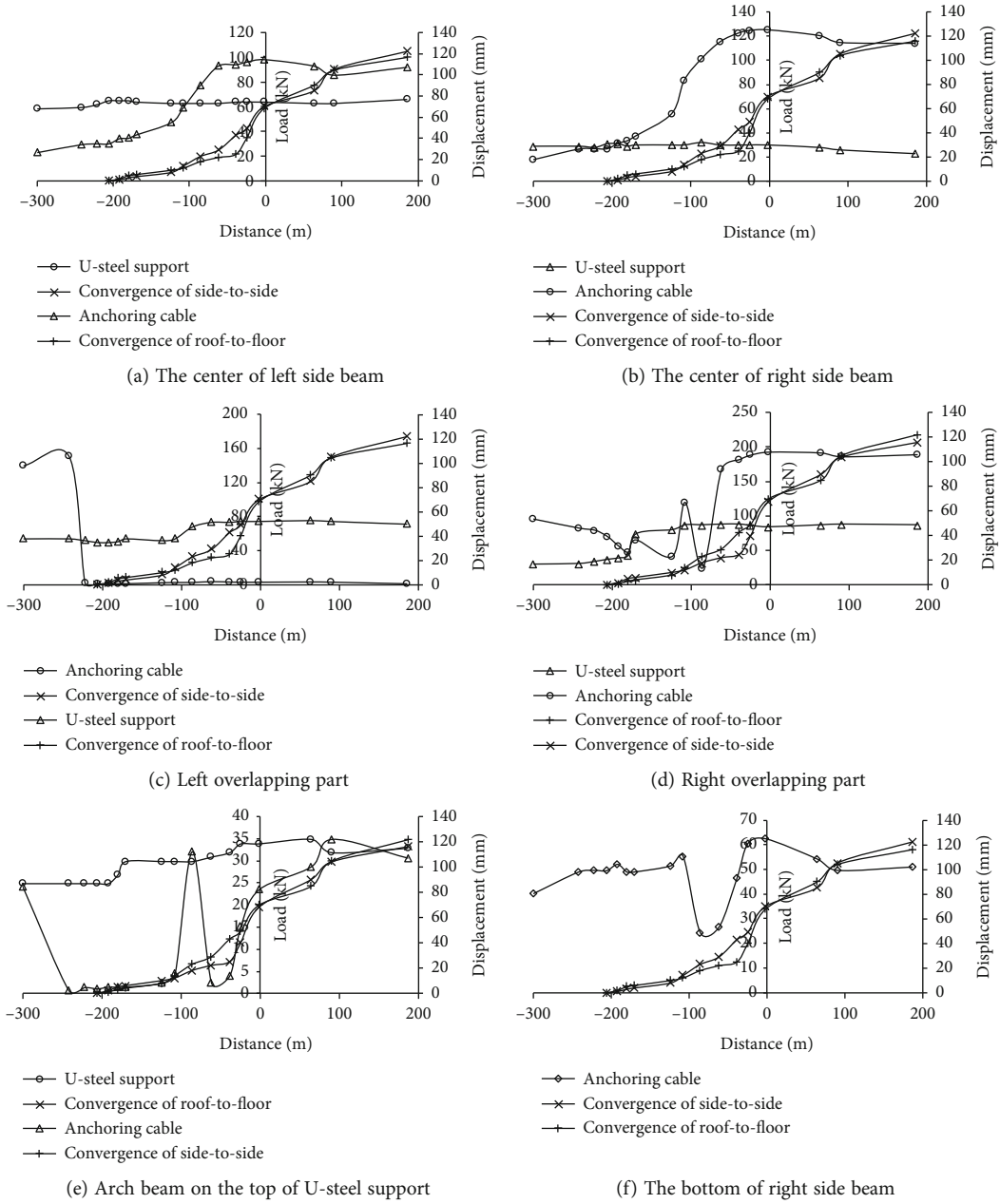(f) The bottom of right side beam

FIGURE 12: Load development of the U-steel support and anchored cables.

the variation tendencies of load of anchored cables are similar to that of convergence of roadway. The maximum load (98 kN) is observed by a pressure cell installed in the center of the left side beam. Meanwhile, the load of the right side beam center is increased from 20 kN to 125 kN. From the previous phenomenon, both side beams are deformed gradually with the side-to-side convergence to release portion overload of U-steel support. The anchored cables become the main bearing body with their loads rising to restrain the oversize deformation of side beams and keep their loads stable. As a result, the violent deformation of surrounding rock is confined effectively by a combined manner of U-steel and anchored cables.

While the monitoring station is behind the working face in the advancing direction of working face, the loads of anchored cables in both side beams are decreased in a small extent. However, during the increasing to 90 m of distance between monitoring station and working face, the loads of two anchored cables are decreased in a small rate. Afterwards, the loads of cables were kept almost constant.

Figure 12(c) shows the relationship between the load of left overlapping part of U-steel support and that of the anchored cables during the deformation of roadway. The load of left overlapping part is changed from 55 kN to 75 kN at the beginning of influence of mining-induced stresses, and it was stable afterwards. However, the anchored

cable is pretensioned with a load of 140 kN in the initial period. And then, the load of anchored cable is suddenly lessened to about zero behind an increased load of 18 kN and keeps below 5 kN. The reason of the phenomenon is analyzed as follows. There is sliding with friction in the left overlapping part to release the sinking movement of arch beam of U-steel support. And the left overlapping part is moved towards to the center of cross-section of roadway. The load of anchored cable is increased up to 158 kN so as to confine the overlapping part without movement. So, bending deflection is generated in the left overlapping part due to continuous deformation of left side beam and arch beam. The symmetry axis of bending deflection is located in the center of the overlapping part. The interval between the support and rock is smaller than that of the initial period result in decreasing the elongation and load of anchored cable in the left overlapping part. After that, there is no obvious increasement of the interval so as the load of anchored cable with a value below 5 kN.

The load developing process of right overlapping part of U-steel support and anchored cable is shown in Figure 12(d). The load of the right overlapping part of U-steel support is gradually increased from below 50 kN to about 80 kN and then tended towards stability. However, the load of the anchored cable is changed in fluctuation to indicate that the sliding and deformation of the right overlapping part is the most evident. From the beginning of load monitoring, there are three decreasing stages due to the declining of interval between support and rock. The reason of that has been explained. The increasing stage is generated after every decreasing stage. And the maximum load of anchored cable (192 kN) is appeared when the working face is located above the monitoring station. The phenomenon is caused by sliding and deformation of the right overlapping part of U-steel support. When the right overlapping part has been sliding, it has generated the movement to the center of roadway cross section and the interval between the support and rock is enlarged. Afterwards, the load of anchored cable is tended to be stable so as that the violent deformation of the right overlapping part of U-steel support is confined.

Figure 12(e) shows the load features of the arch beam and that of the anchored cable. The load of arch beam of U-steel support is constantly increased from 25 kN to about 35 kN. While the monitoring station is behind the working face in the advancing direction of working face, the load of arch beam was kept above 30 kN. However, the load of anchored cable is observed in a tendency with decreasing-increasing-decreasing-increasing stability. In the first stage, the convergence of side-to-side roadway is larger than that of roof-to-floor so as to make the center part of arch beam upward. The interval between it and the rock is smaller than that in the initial situation. So, the load of anchored cable is lessened from the start at 25 kN to below 5 kN. And the load remained at below 5 kN for a long time. When the working face is 90 m in front of the monitoring station, the load of the anchored cable is increased to 35 kN due to the sinking movement of the arch beam. At the same time, it is found that the load of anchored cable installed right overlapping part of the U-steel support is dramatically reduced by com-
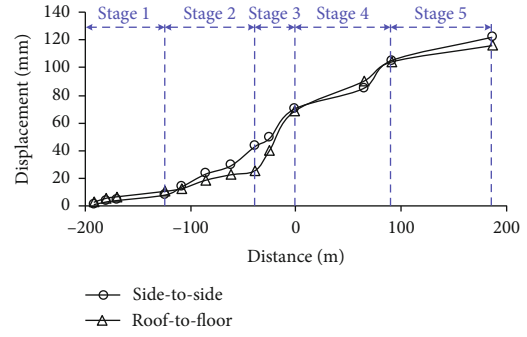

Figure 13: Developing process of deformation of test roadway.

paring with Figure 12(d). And then, it is correct that the bending deflection of the overlapping part of U-steel support is generated by the sinking movement of the arch beam. Afterwards, the load of anchored cable in the arch beam is lessened again, while that of the anchored cable in the right overlapping part of U-steel support is increased. Although there is some sinking of arch beam, the convergence of side-to-side is larger to compress and raise the center of arch beam again. Meanwhile, the raising movement is promoted by the sliding and deformation of right overlapping part of U-steel support. Therefore, the interval of between support and rock is smaller than that in the previous stage result in reducing the load of the anchored cable. In the following stages, the load of the anchored cable is gradually increased to 35 kN with a tendency similar to that of roadway deformation during the variation of distance between monitoring station and working face.

Figure 12(f) shows the relationship between the convergences of roadway with the load of anchored cable installed in the bottom of the right side beam. The load of the anchored cable is gradually increased from 48 kN to 57 kN. When the monitoring station is 90 m in front of the working face, the load of the anchored cable is dropped below 30 kN. Along with a constant increasing of roadway deformation, the load of the anchored cable is increased to the maximum of 63 kN. When the working face is about 90 m in front of the monitoring station, the load of the anchored cable is reduced in a small extent and was kept constant in the following time.

8. Discussions

(1) The stages, extent, and scope of influence of mining-induced stresses: as shown in Figure 13, the deformation of the -720 south-wing track haulage roadway can be divided into 5 stages: stable deformation without mining influence (stage 1), slight deformation under advanced mining influence (stage 2), severely deformation under advanced mining influence (stage 3), slight deformation after mining influence (stage 4), and stable deformation after mining influence (stage 5). The developing process of roadway deformation is also reflected by the load features of USS-AC due to mining-induced stresses. Therefore, according to the space relationship
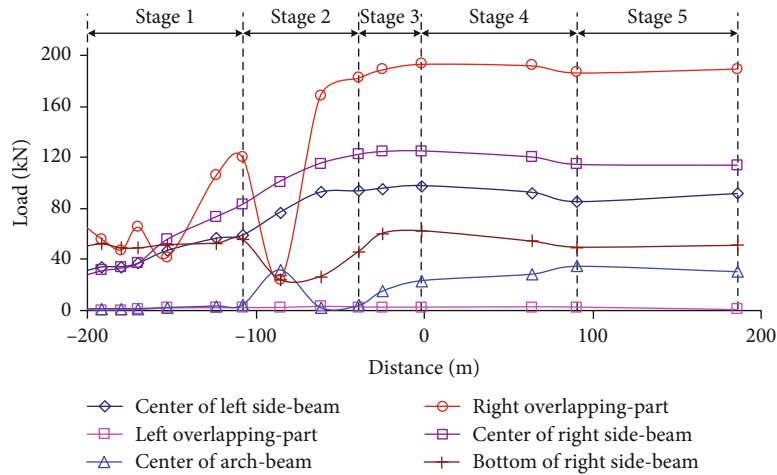
FIGURE 14: Load development of anchored cables.

between test roadway with working face II7$_2$14 and the geological conditions, the scope of advanced abutment pressure caused by the working face is about 140 m. And the influencing scope behind the working face is in a range of 80 m-90 m. The changing law of mining-induced stresses is essential to select the implementing time of extra reinforcing measures of roadway similar to the previous conditions.

(2) The bearing characteristics and implementing locations of anchored cables: in sum, the supporting resistance generated by USS-AC is applied to control the deformation of the -720 south-wing track haulage roadway during the excavation of working face II7$_2$14. The load of U-steel support is kept stable due to the restraining action of the anchored cables. However, the anchored cables installed in the right overlapping part and the center of two side beams are the main bearing bodies with high loads during the stage 3. And in this stage, the convergence of side-to-side of test roadway is larger than that of roof-to-floor. The influencing extent of mining pressure of the side wall of test roadway is heavier than that of the roof. If those anchored cables are removed, the destruction of U-steel support is generated in the right overlapping part and the center of two side beams firstly. Therefore, it can be seen that the anchored cables offer an extra load to optimize the bearing characteristics of U-steel support and increasing the load limit of collaborative reinforce system to confine the deformation of roadway. The changing law of USS-AC loads is significant to select the implementing location of extra reinforcing measures of roadway similar to the previous conditions.

(3) The deformation features and sliding movements of U-steel support: the anchored cables are contacted with U-steel support by joists. The load features of anchored cables are the direct reflection of the defor-

mations or movements of different parts of U-steel support. As shown in Figure 14, in accordance to the cable load, each side beam of the U-steel support is displaced towards the space of test roadway at the 5 stages. The deformation of arch beam on the top is in a procedure of upward-downward-upward-downward. Analyzing the procedure, the upward movement with bending is generated at the center of arch beam because of continuous displacement of both side beams. Afterwards, there is downward movement of the entire arch beam. The deformation of overlapping part which includes sliding movement and bending deformation is related to that of arch beam and side beams. Among it, the bending deformation of overlapping part is produced to lessen the load of anchored cable under the sinking deformation of entire arch beam at the 2nd stage. Meanwhile, when the rock near to the overlapping part and side beam is displaced, there is sliding movement of overlapping part leading to increase the load of anchored cable. The deformation law of different segments of U-steel support is revealed by qualitatively inverse analysis of loads of anchored cables. The results are useful to optimize the installing location of extra anchored cables.

However, there are several issues to be studied as follows: (a) quantitative analysis on the loads relationship between U-steel support and anchored cables by using a theoretical model and (b) building a precisely numerical model of U-steel support and analyzing its response characteristics under various conditions of load.

9. Conclusions

(1) The distribution of stress in the surrounding rock is changed to increasing the residual strength of rock near to the space of roadway by using USS-AC. The extra supporting resistance is supplied by

anchored cables to optimize the moment distribution and enhance the nondeformability and the global stability of the U-steel support. And then, the deformation of roadway is significantly restrained. According to the result of monitoring, both the convergence of side-to-side and that of roof-to-floor are below 120 mm to satisfy the requirement for usefulness of test roadway during the influence process of mining-induced stresses

(2) According to the loads of anchoring cables, the high deformation loads are generated at the right overlapping part and the centers of two side beams undergoing severe mining-induced stresses. And, the anchoring cables are the main bearing bodies with supporting resistance above 100 kN to control the displacement of the right overlapping part and two side beams of U-steel support. Increasing load limit and stiffness of side beams are significant to enhance the bearing ability of arch beam

(3) As an integral structure, the U-steel support is confined to the limited deformation space owing to extra action of anchoring cables. Excessive deformations of arch beam and side beams are released through the sliding movements of overlapping parts of U-steel support so to realize the properties of high resistance and contractibility of the U-steel support

Data Availability

The data is from the project of Renlou Coal Mine in the north of Anhui Province of China.

Conflicts of Interest

The authors declare that they have no conflicts of interest.

Acknowledgments

References

[1] H. P. Kang, G. F. Wang, P. F. Jiang et al., "Conception for strata control and intelligent mining technology in deep coal mines with depth more than 1000m," *Journal of China Coal Society*, vol. 43, no. 7, pp. 1789–1800, 2018.

[2] H. P. Kang, P. F. Jiang, J. W. Yang et al., "Roadway soft coal control technology by means of grouting bolts with high pressure-shotcreting in synergy in more than 1000m deep coal mines," *Journal of China Coal Society*, vol. 46, no. 3, pp. 747–762, 2021.

[3] C. J. Hou and P. F. Gou, "Mechanism study on strength enhancement for the rocks surrounding roadway supported by bolt," *Chinese Journal of Rock Mechanics and Engineering*, vol. 19, no. 3, pp. 342–345, 2000.

[4] N. Zhang and M. S. Gao, "High-stress and pretension bolting support of coal roadway and its application," *Journal of China University of Mining and Technology*, vol. 33, no. 5, pp. 524–527, 2004.

[5] H. P. Kang and J. H. Wang, *Rock Bolting Theory and Complete Technology for Coal Roadways*, China Coal Industry Publishing House, Beijing, 2007.

[6] H. P. Kang, J. Lin, Y. Z. Wu, P. Cheng, X. Z. Meng, and S. Ren, "Mechanical performances and compatibility of rock bolt components," *Journal of China Coal Society*, vol. 40, no. 1, pp. 11–23, 2015.

[7] H. P. Kang, P. F. Jiang, B. X. Huang et al., "Roadway strata control technology by means of bolting-modification-destressing in synergy in 1000m deep coal mines," *Journal of China Coal Society*, vol. 45, no. 3, pp. 845–864, 2020.

[8] W. B. Xie, S. G. Jing, T. Wang, Y. K. Ren, and N. Zhang, "Structural stability of U-steel support and its control technology," *Chinese Journal of Rock Mechanics and Engineering*, vol. 29, no. S2, pp. 3743–3748, 2010.

[9] S. G. Jing, *Study on Control Mechanism of Cooperating Support of Support and Anchored Cable in Soft Fragmentized Surrounding Rock Roadway with High Stress [Ph. D. Thesis]*, China University of Mining and Technology, Xuzhou, 2009.

[10] Q. Z. Wang, W. B. Xie, S. G. Jing, L. Zang, and N. Zhang, "Research on U-shape steel frame anchor cable collaborative support mechanism and loading law of roadway under dynamical pressure impact," *Journal of China Coal Society*, vol. 40, no. 2, pp. 301–307, 2015.

[11] C. A. You, "Stability analysis of U-steel yieldable support," *Chinese Journal of Rock Mechanics and Engineering*, vol. 21, no. 11, pp. 1672–1675, 2002.

[12] C. A. You, "Internal force calculation of U-supports considering yielding," *Chinese Journal of Geotechnical Engineering*, vol. 22, no. 5, pp. 604–607, 2000.

[13] J. Z. Liu, N. Zhang, X. G. Zheng, and B. G. Wang, "Research on buckling failure mechanism of U type steel support loaded deviating longitudinally," *Journal of Coal Science & Engineering*, vol. 36, no. 10, pp. 1647–1652, 2011.

[14] C. A. You, *Computing Theory on Steel Support of Roadway*, China Coal Industry Publishing House, Beijing, 2000.

[15] L. Tian, W. B. Xie, S. G. Jing, Y. D. Xing, and J. P. Peng, "Framed timber and anchor coupling collective support technology for fully mechanized top coal mining face crossing over gateway," *Coal Science and Technology*, vol. 39, no. 11, pp. 44–47, 2011.

[16] D. H. Wang, H. R. Guo, H. Zhao, and Y. W. Guo, "Analysis of influences of weak joints and confining pressure on rock-mass strength by numerical simulation," in *Applied Mechanics and Materials*, vol. 438, pp. 607–611, Trans Tech Publications, Ltd., Oct, 2013.

[17] Y. Gan, S. Gan, and X. Zhen, "Study of the influence of joint on the triaxial compression strength," *Science Technology and Engineering*, vol. 12, pp. 9861–9864, 2012.